ATMIRE

Title	Geophysical interpretation of development of Tertiary structure in the Gulf of Panama Basin
Item Type	Text
Authors	Marshall, David B.
Publisher	Colorado School of Mines. Arthur Lakes Library
Rights	Copyright of the original work is retained by the author.
Download date	2026-11-28 03:00:24
Link to Item	https://hdl.handle.net/11124/175937

T 1792

GEOPHYSICAL INTERPRETATION OF DEVELOPMENT OF TERTIARY STRUCTURE IN THE GULF OF PANAMA BASIN

by

David B. Marshall

12703-86

ProQuest Number: 10782006

All rights reserved

INFORMATION TO ALL USERS
The quality of this reproduction is dependent upon the quality of the copy submitted.

In the unlikely event that the author did not send a complete manuscript and there are missing pages, these will be noted. Also, if material had to be removed, a note will indicate the deletion.



ProQuest 10782006

Published by ProQuest LLC (2018). Copyright of the Dissertation is held by the Author.

All rights reserved.
This work is protected against unauthorized copying under Title 17, United States Code
Microform Edition © ProQuest LLC.

ProQuest LLC.
789 East Eisenhower Parkway
P.O. Box 1346
Ann Arbor, MI 48106 – 1346

T 1792

A Thesis submitted to the Faculty and the Board of Trustees of the Colorado School of Mines in partial fulfillment of the requirements for the degree of Master of Science (Geophysics).

Signed: David B. Marshall
David B. Marshall

Golden, Colorado

Date: Dec. 5, 1975

Approved: Tom L. Davis
Tom L. Davis
Thesis Advisor

George V. Keller
G. V. Keller
Head of Department

Golden, Colorado

Date: DEC. 8, 1975

ABSTRACT

The Gulf of Panama Basin lies at the northern end of the Bolivar Geosyncline of the Pacific margin of northern South America. The basin contains sediments of Eocene to Pliocene age, deposited in a system of horst and graben sub-basins that includes the basins of the on-shore area of eastern Panama.

The Gulf of Panama can be divided into two distinct parts as determined from stratigraphic information from the Corvus #1 and Plaris #1 wells (Figure 1) and from interpretation of 1700 miles of seismic data. The western part of the basin contains sediments of Eocene age with high densities (2.5-2.9 g/cc), high seismic velocities (11000-15000 fps) and high percent of volcanic rocks buried at shallow depth (1000-2500 feet). The Eocene rocks have been deformed by igneous intrusion and vertical movements within the basement, eroded, and covered by a veneer of Pliocene and younger rocks.

The eastern part of the basin contains Miocene and younger rocks deposited with only a short period of interruption at the end of Middle Miocene time as evidenced by truncation of Middle Miocene rocks by overlying Late Miocene rocks on the structure drilled by the Plaris #1 well.

The seismic data and the high velocity and density of Eocene rocks in the western part of the basin, indicate that the western part of the basin once contained Miocene sedi-

ment which buried the Eocene sediment at great depth. Subsequent uplift, probably coincident with the Middle Miocene uplift on the eastern basin, resulted in the erosion of Miocene sediments from the entire area of the western part of the basin.

The horst and graben nature of the Gulf of Panama basin, the Middle Miocene age of structure formation, and the nature of the stratigraphic sequence in the basin are all distinctly recognized characteristics in the basins onshore eastern Panama. Therefore, the Gulf of Panama basin can be grouped with the basins onshore eastern Panama as part of the Bolivar Geosyncline.

COLORADO SCHOOL OF MINES LIBRARY

TABLE OF CONTENTS

	Page
INTRODUCTION	1
PURPOSE AND SCOPE OF INVESTIGATION	3
Objective	3
Area of Study	3
Stratigraphy	4
Structure	5
INVESTIGATION PROCEDURE	7
Seismic Data	7
Gravity and Magnetic Data	8
Well Data	9
INTERPRETATION	12
Time Structure Maps	12
Regional Features	12
Time of Structure Development	13
Forces of Structural Development	15
Periods of Folding and Faulting	16
Unconformities	16
Gravity Data	17
Total Magnetic Intensity Data	20
Seismic Velocities	22
Interpretational Limitations	29
PLATE TECTONICS	31
CONCLUSIONS	34
BIBLIOGRAPHY	37

LIST OF FIGURES

Figure		Page
1.	Location Map	2
2.	Stratigraphic Column	10
3.	Seismic Structure Map, Eocene-Middle Miocene Horizon	14
4.	Bouguer Gravity Map	18
5.	Total Intensity Magnetic Map	21
6.	Calibrated Velocity Log	27
7.	Plate Motion	33

LIST OF PLATES (author did not furnish Plates.

I.	Seismic Structure Map Eocene-Middle Miocene Horizon (2 Sheets)	In Pocket
II.	Seismic Structure Map Pliocene-Middle Miocene Horizon (2 Sheets)	In Pocket
III.	Seismic Line 33	In Pocket
IV.	Seismic Line 19	In Pocket
V.	Seismic Line 42	In Pocket
VI.	Seismic Line 59	In Pocket
VII.	Seismic Line 32	In Pocket
VIII.	Seismic Line 26	In Pocket

LIST OF TABLES

Table		Page
1.	Gravity and Magnetic Features	23
2.	Plaris #1 Velocity Summary.	24
3.	Corvus #1 Velocity Summary.	25
4.	Velocity Analysis Calibration	28
5.	Sedimentary and Tectonic Events	36

T 1792

ACKNOWLEDGMENTS

The seismic, gravity, magnetic, and well log data used in this thesis were provided by the following companies:

El Paso Natural Gas, Oceanic Exploration, Great Plains Development, Sante Fe International, Pacific Lighting Gas Development, and Mono Power. I would like to thank these companies for their cooperation, which made this study possible.

I would like to thank the American Smelting and Refining Company for providing financial support through the ASARCO Foundation Fellowship during part of my graduate study.

INTRODUCTION

The Gulf of Panama is located in the transition zone between the South American Continent geologic province and the nuclear Central America geologic province. These two provinces have evolved under separate but related tectonic environments. Knowledge of the age and mechanisms of structural development in the Gulf of Panama will aid in the understanding of the regional geology of Central America and help provide a more complete and unified picture of the geology in this region.

The problem to be solved is: by what mechanism did the structure of the Gulf of Panama basin form and at what time in geologic history? The answer to this question will be formulated through the examination of reflection seismic records and maps and Bouguer gravity and total magnetic intensity maps.

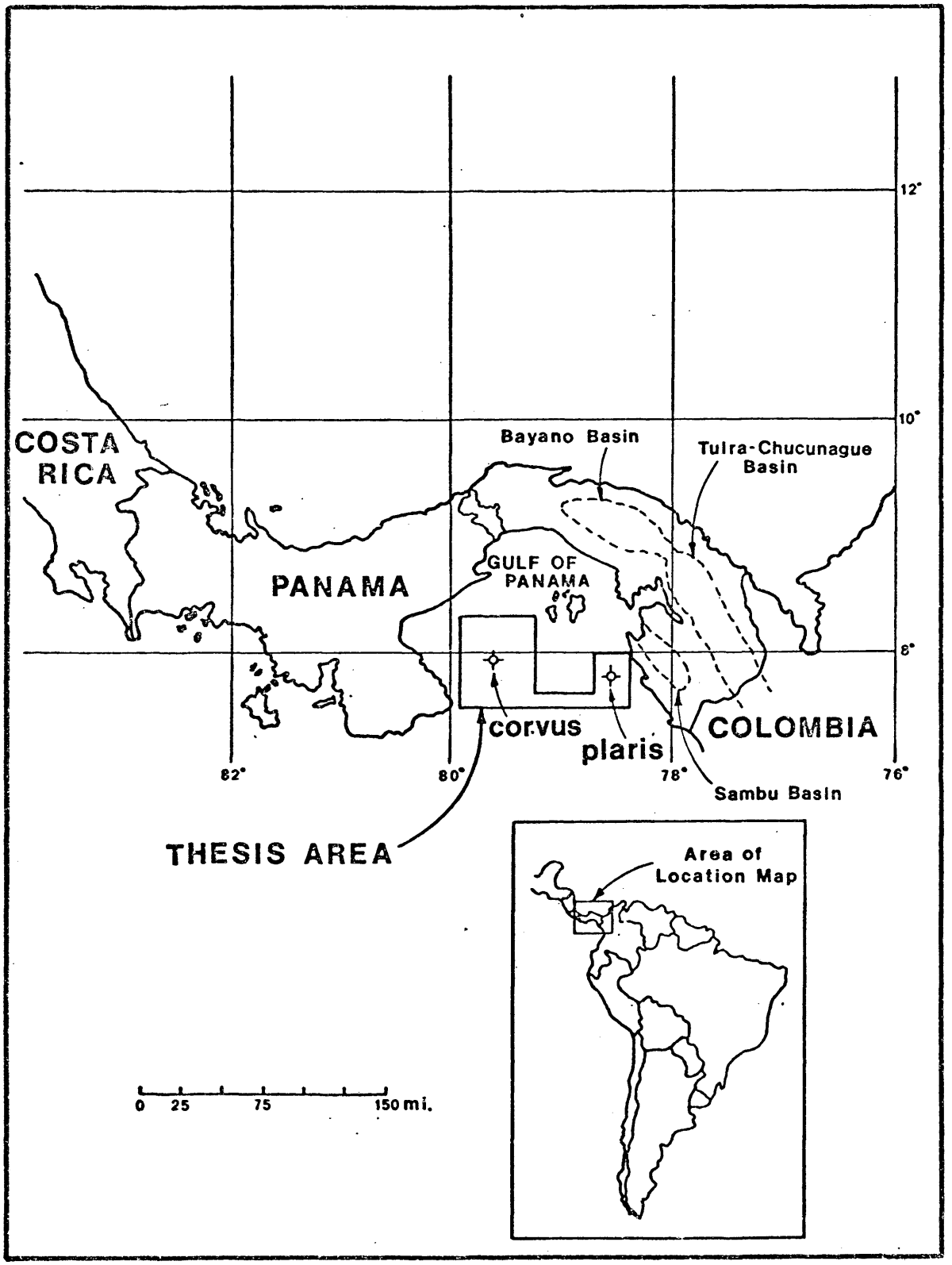


FIGURE 1: LOCATION MAP

PURPOSE AND SCOPE OF INVESTIGATION

Objective

In determining the age and mechanism of structure development, the following factors will be considered:

Regional distribution of folds and faults

Evidence of compressional or tensional forces in structure development

Relative ages of folds and faults

Time correlation for different periods of folding and faulting

Ages and types of unconformities.

Individual structural features will be examined according to these five characteristics and the structural history of the basin will be summarized.

Area of Study

The area of study as shown in Figure 1 lies to the south of the isthmus of Panama. The area covered by the available seismic data is approximately 2600 square miles. This area encompasses essentially all of that part of the Gulf of Panama which contains Tertiary sediments.

The isthmus of Panama consists of two separate geologic provinces which border along a line coinciding approximately with the Panama Canal. East of the canal lies the basins of the northern end of the Bolivar Geosyncline which extends southward into western Colombia. West of the canal is the volcanic province of the archipelago of south Central

America. Eastern Panama is an appendage of the South American continent which has been connected to nuclear Central America by this volcanic archipelago which began developing during Middle Oligocene. The Tertiary volcanics of the archipelago completely cover the older rocks in western Panama so that nothing is known of Pre-Tertiary history of this area.

Stratigraphy

The basins of the Bolivar Geosyncline contain marine, shallow marine and terrestrial sediments of Eocene to Pliocene age. Each basin occupies an elongate graben and is separated from other basins by a horst block which prevented the transport of sediments from one basin to another.

Three basins were formed in eastern Panama during Tertiary time. The Bayanu and Tuira Chucunague basins are in central eastern Panama and extend to the south across the Colombian border. The Sambu Basin is southwest of the Bayanu and Tuira Chucunague basins and extends into the Gulf of Panama.

The oldest sedimentary rocks that accumulated in the basins are Eocene in age. Active sedimentation in the basins continued through Pliocene time with a total known accumulated thickness of over 20,000 feet (Johnson and Headington, 1971).

Those rocks underlying the Eocene sediments are interbedded volcanics and sediments probably of Cretaceous or

Eocene age. The pre-Cretaceous history of Panama is unknown since no rocks older than Cretaceous have been found (Johnson and Headington, 1971).

Sediment deposition within the basins began with the formation of the Bolivar Geosyncline during Eocene time when volcanic pyroclastics and agglomeratic rocks were supplied to the basins. Marine transgression increased within the Bolivar Geosyncline in Oligocene marked by a general end to the volcanic activity. The sedimentation continued through Early Miocene time. During Middle Miocene time, diastrophic uplift and erosion occurred forming the coastal and interior mountain ranges and producing the fold and fault systems that are observed today.

Structure

Panama is underlain by a faulted intrusive core of probable Laramide age (Johnson and Headington, 1971). Tectonic movement within this core has localized the accumulation of sediments by producing boundaries between sedimentary basins. The boundaries are elongate horst blocks with the basins occupying the intervening grabens.

These basins have elongate axes that trend N35^{o}W. Folds and faults in the basins trend N35^{o}W and N50^{o}E. The structure began to develop in Middle Miocene time. The major structural features appear regionally as a series of arcs, convex to the north cut by a series of faults radially intersecting the concentric structures.

At least one angular unconformity has been identified between Middle Miocene and older rocks.

INVESTIGATION PROCEDURE

To aid in discussing the study area, the Gulf of Panama will be divided into two areas that will be referred to as the eastern part of the basin and the western part of the basin. The eastern part of the basin is the area east of seismic line 24 and the western part is west of this line. This division does not mean that two separate basins existed in the study area in Tertiary time but provides a geographic boundary that is useful in discussing the stratigraphic and structural variations in the Gulf of Panama.

Seismic Data

1713 miles of reflection seismic data have been used in construction of the seismic time maps. These data were acquired in 1971 and 1972 by Western Geophysical Company. Data from the 1971 survey were processed with a 12-fold common depth point stack and were deconvolved before and after stacking with a final time-varying filter applied. Data from the 1972 survey were processed with a 24-fold common depth point stack and were deconvolved before and after stacking with a final time-varying filter applied.

Seismic structure maps were prepared on two horizons which illustrate the structure within the Tertiary sediments. The shallowest horizon mapped is of Pliocene and Middle Miocene age. This horizon corresponds approximately with a widespread angular unconformity that developed sometime near

the end of Middle Miocene time or beginning of Late Miocene time. Below this unconformity, horizons are mapped which illustrate the structure developed prior to deposition of Late Miocene and Pliocene sediments. Both maps are contoured on an interval of .05 second with index contours each .25 second.

The quality of the seismic reflection data varies greatly between the eastern part of the basin and the western part. In the eastern part, coherent mappable reflections are present at reflection times below 2.0 seconds. In the western part of the basin, coherent reflections are seldom seen below 2.0 seconds and there is no reflection event below the Pliocene-Late Miocene age unconformity that can be reliably mapped over the entire basin. Therefore, the Eocene horizon map of the western part of the basin depicts the structure within the basin but does not permit the projection of stratigraphic information from the Corvus #1 well to other parts of the basin.

Gravity and Magnetic Data

1056 miles of gravity and magnetic data were collected during the seismic survey of 1971. These data were prepared and interpreted by EDCON Company of Denver, Colorado. EDCON prepared Bouguer gravity, depth to basement, and total magnetic intensity maps. The gravity and magnetic maps of Figures 4 and 5, are taken from the maps prepared by EDCON.

Well Data

Two dry wells were drilled in the Gulf of Panama in 1974. On March 26, 1974 the Corvus #1 well was completed at a total depth of 8625 feet. On May 21, 1974 the Plaris #1 well was completed at a total depth of 9408 feet. A velocity survey was made in each well by raising a geophone in the well and using an airgun to produce a seismic signal when the geophone reached certain depths. The velocity data was processed by Birdwell Division of Seismograph Service Company and calibrated velocity logs giving integrated travel time and interval velocity were prepared. The velocity surveys were used to correlate the stratigraphic section with the reflection times on the seismic sections.

The Corvus and Plaris wells also provide accurate dating of the Tertiary sedimentary section and identification of the lithologies. As shown in Figure 2, a major regional angular unconformity exists between Pliocene to Late Miocene and older sediments. In the Corvus well, the unconformity is between Middle Eocene and Pliocene age sediments. In the Plaris well the unconformity is between Middle Miocene and the base of Late Miocene age sediments. In the western part of the basin, erosion continued through Late Miocene, or repeated uplift resulted in the removal of any Miocene sediments deposited in this area.

The Eocene sediments are described on the mud log as predominantly volcanic derived sands, conglomerates and tuffs very similar to published descriptions of Eocene and

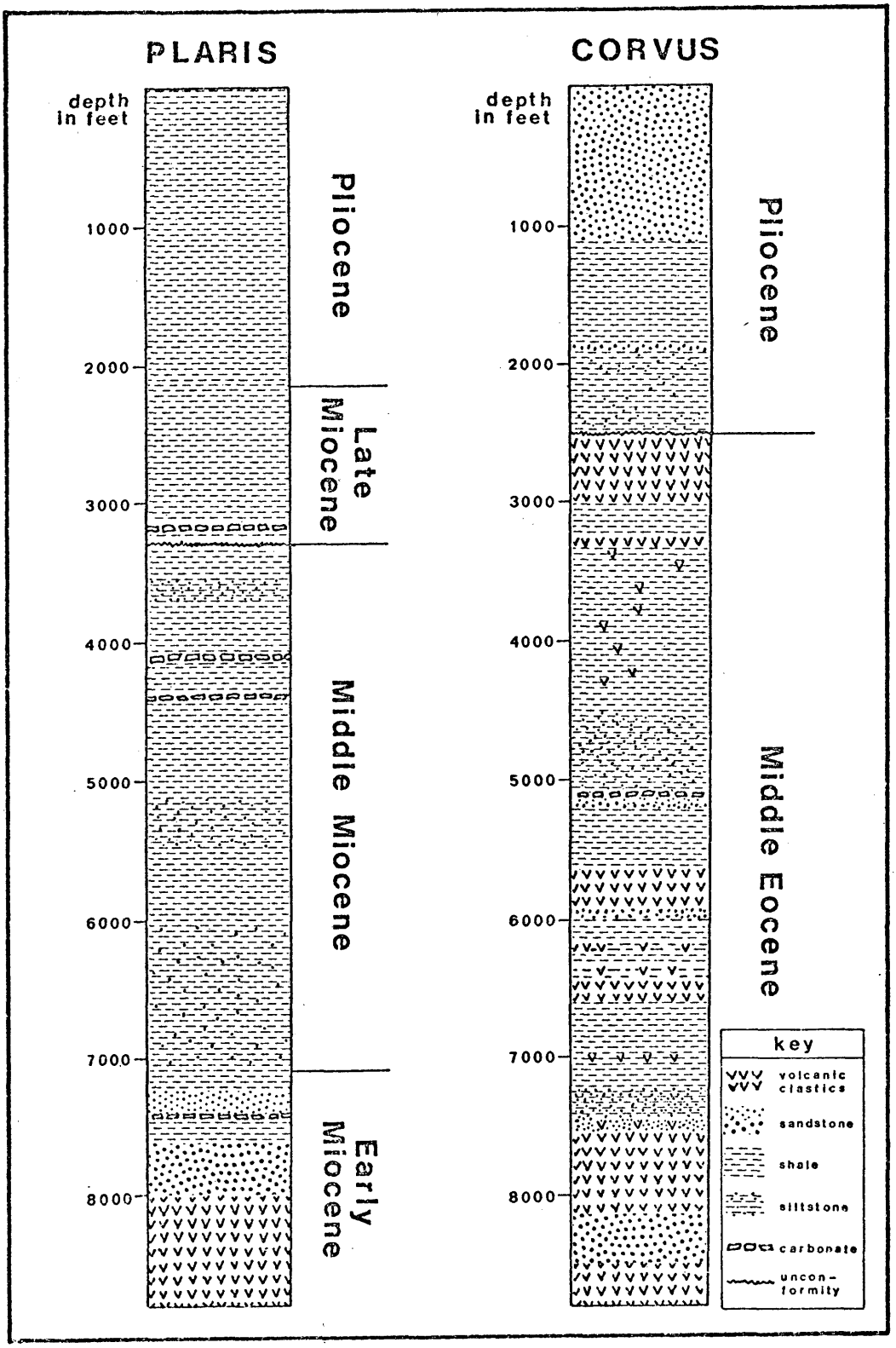


FIGURE 2: STRATIGRAPHIC COLUMN

Oligocene rocks of the basins onshore in eastern Panama (Johnson, et al., 1971; Terry, 1956). The Miocene sediments from the Plaris well are marine sands and shales with thin carbonates. A highly volcanic section is present from 8000 feet to total depth in the Plaris well. The age of this section is Early Miocene. This provides an accurate date to the end of volcanic sedimentation in eastern Panama.

INTERPRETATION

Time Structure Maps

Regional Features

The two time structure maps, Plates I and II, show several important regional features of the basin. In the western basin is an elongate east-west trending graben lying along the southern border of the study area. The north and south bounding faults of this graben have no expression in the sediments above the Pliocene-Miocene unconformity, thereby restricting the age of the faults to pre-Pliocene. The faults appear to extend at depth into the basement. The fault graben nature of this basin indicates that it is similar to the eastern part of the Gulf of Panama basin and the basins onshore eastern Panama.

Within the graben are approximately 3000 feet of sediments between the Eocene mapping horizon and the unconformity. The velocity of the sediments below the unconformity is over 12,000 feet per second, indicating that these sediments are similar in lithology to the sediments below the unconformity in the Corvus well. There is no indication on the seismic lines that the bounding faults were active during deposition of the sediments below the unconformity.

North of this graben is a west plunging anticline, faulted on the south and west by the north bounding fault of the graben. Movement on this bounding fault, shotpoint 645, line 32 (Plate VII), occurred after deposition of Eocene

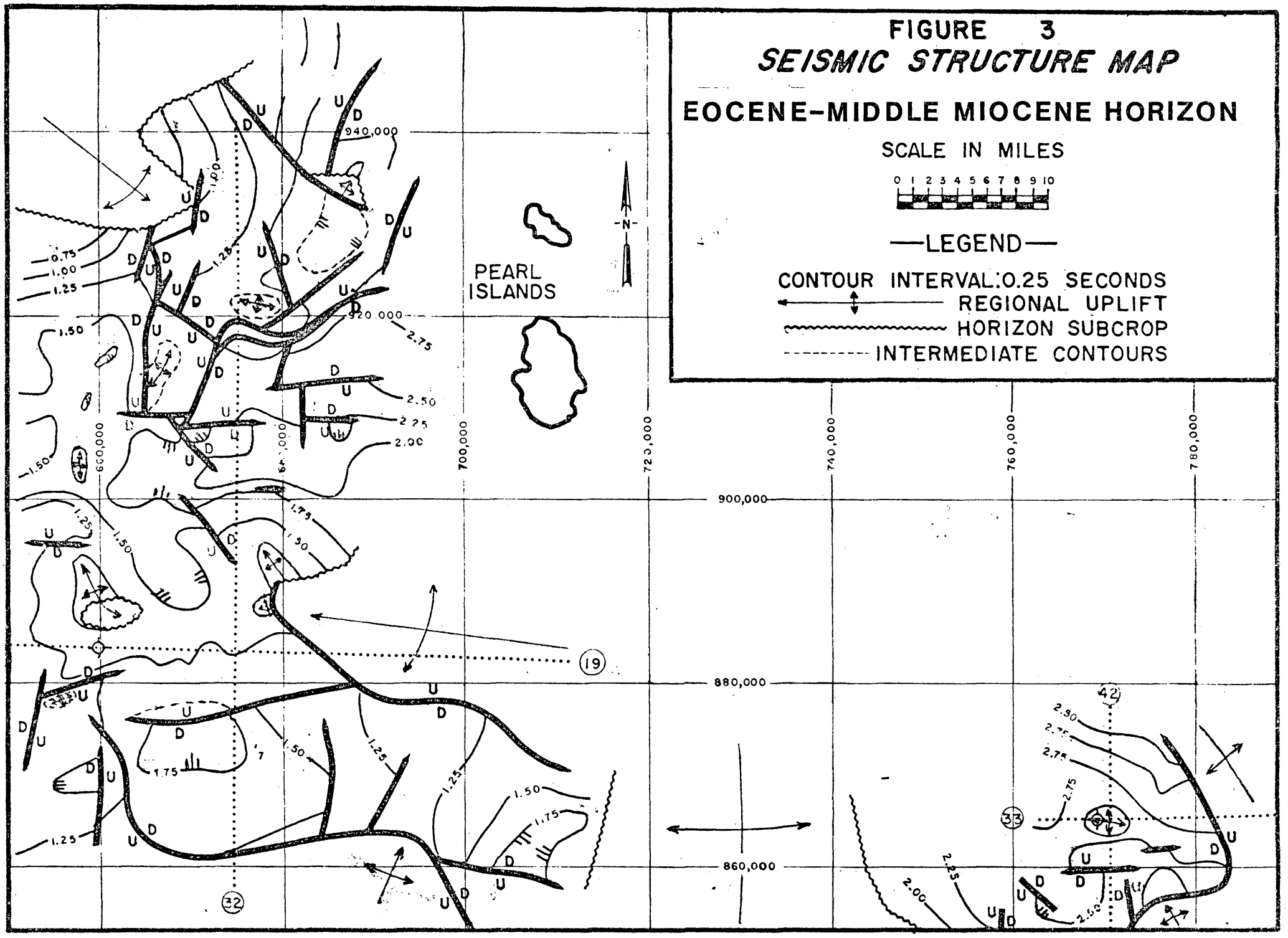
sediments. However, the sedimentary section on the north flank of this anticline, shotpoint 300 to shotpoint 500, line 32, increases in thickness from south to north. This anticline was forming or existed while the sediments on its north flank were being deposited. Therefore, to the north of the anticline is a separate depositional basin.

In the northwest corner of the study area is another large anticlinal uplift which plunges to the east (Figure 3). This anticline and the anticline and graben in the southern part of the study area define a regional east-west structural trend. A north-south regional structural trend is defined by the two anticlinal uplifts along the southern edge of the study area (Figure 3).

The eastern part of the basin is a graben which parallels the graben basins of onshore eastern Panama. Stratigraphic age correlations from the Plaris well show that this graben began forming at least as early as Early Miocene and has continued to subside through Pliocene (plate III). The geometry and age of this graben indicate that it is similar to the basins onshore Panama and is therefore interpreted as the offshore extension of the onshore horst and graben basin system.

Time of Structure Development

In general, all structure in both parts of the basin formed prior to the deposition of sediments above the unconformity between Late Miocene and older sediments. Seismic


FIGURE 3
SEISMIC STRUCTURE MAP
EOCENE-MIDDLE MIOCENE HORIZON
SCALE IN MILES
0 1 2 3 4 5 6 7 8 9 10
—LEGEND—
CONTOUR INTERVAL: 0.25 SECONDS
REGIONAL UPLIFT
HORIZON SUBCROP
INTERMEDIATE CONTOURS
PEARL ISLANDS
N
940,000
920,000
900,000
880,000
860,000
600,000
640,000
700,000
720,000
740,000
760,000
780,000
19
32
33
42

lines 33, 19, 42, 59, 32 and 26 (Plates III, IV, V, VI, VII, VIII) show that all folding occurred prior to deposition of Late Miocene sediments. Since the oldest sediments at the unconformable surface are of Eocene age and the youngest sediments are of Middle Miocene and Pliocene age, the structural development could have started as early as Eocene time and must have ceased by the beginning of Late Miocene time. The lack of growth faulting or other indications of structure development contemporaneous with deposition of Eocene sediments points to a Post-Eocene age of structure development. This is consistent with the onshore basins of eastern Panama in which the structural development began in Middle Miocene time.

On line 33 (Plate III), the structure on which the Plaris well was drilled exhibits thinning of the Middle Miocene section across the top of the structure. This indicates that structure in the Gulf of Panama began developing during Middle Miocene as did the structure onshore eastern Panama.

Forces of Structural Development

All faulting in the basin is normal faulting resulting from relative uplift or subsidence of adjacent blocks. However, major faults appear to be of two types:

1. Faults that are associated with development of folds.
2. Faults that bound large uplifted basement blocks.

The first of these fault types is represented by the low angle normal fault that intersects line 32 (Plate IX) at shotpoint 220.

The second of these fault types is represented by the bounding faults of the graben along the southern border of the study area. Two other examples are the faults that intersect line 14 at shotpoint 260 and shotpoint 355 (Plate I).

Nearly all folds and faults resulted from vertical movements which originated in the basement. Only the structure at the intersection of lines 32 and 37 appears to have resulted from flowage of relatively unconsolidated, mobile sediments. The discordance of dips of reflections across this structure indicates that it is either a slump feature or a diapiric feature.

Periods of Folding and Faulting

The anticlinal and synclinal features in the sediments above the unconformity coincide with corresponding anticlinal and synclinal features in the sediments below the unconformity. Plates I, II, and III illustrate this correspondence for the structure on which the Plaris well was drilled. Plates I, II, and VII illustrate this correspondence for the anticlinal uplift and graben in the southern half of the western part of the study area. None of the regional faults bounding horst and graben blocks were active after deposition of post-Middle Miocene sediments.

Unconformities

The regional angular unconformity between Eocene and Middle Miocene to Pliocene sediments is best illustrated on line 42 (Plate V). As seen on this line, the unconformity truncates reflections that occur as deep as 3.0 seconds

in the middle of the basin.

On line 42 at shotpoint 215 (Plate V) is the edge of the area in which Late Miocene sediments are preserved. Deposition of Late Miocene sediments was restricted to the area north and east of this edge.

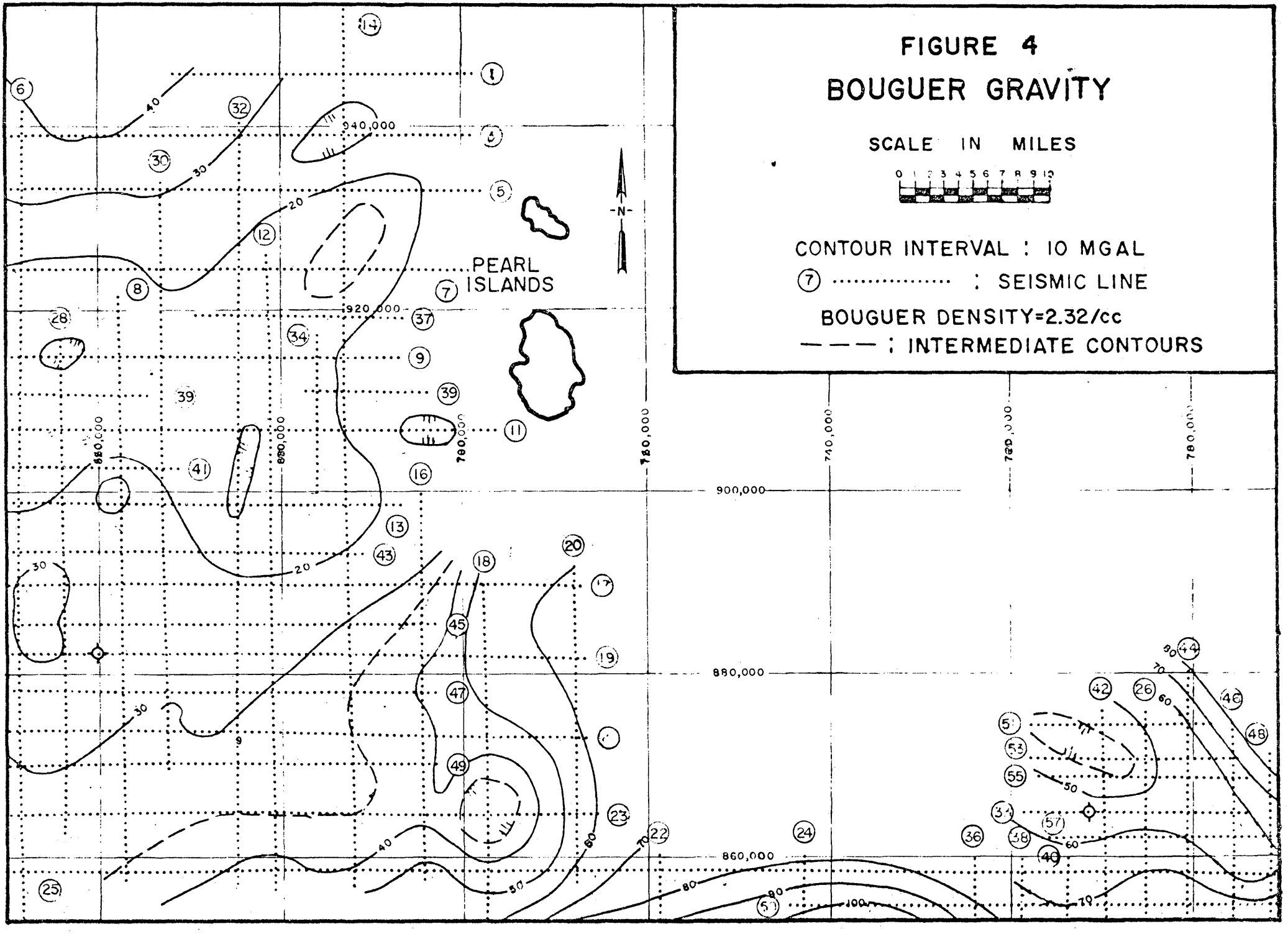
Gravity Data

The Bouguer gravity map (Figure 4) was produced from the data acquired during the seismic survey of 1971. Since the line spacing of this survey is approximately 5 miles, the map represents only gross regional features related to the depth of basement rocks. However, in interpreting the gravity data from this basin it should be noted that the bulk density of the Eocene sedimentary rocks is relatively high. From the bulk density log of the Corvus #1 well, typical densities are:

4000 feet	2.40-2.50 g/cc
4500 feet	2.65-2.80 g/cc
5500 feet	2.45-2.55 g/cc
6000 feet	2.50-2.60 g/cc
6500 feet	2.55-2.65 g/cc
7000 feet	2.45-2.50 g/cc
8000 feet	2.75-2.90 g/cc
8500 feet	2.80-2.90 g/cc

The densities over this 4500 foot interval range from densities generally considered typical of sedimentary rocks (2.40-2.60 g/cc) to densities generally considered to be typical of basement rocks (2.7-2.9 g/cc).

The Bouguer gravity map is contoured on an interval of 10 milligals. Generally, the Bouguer gravity map illustrates the basic configuration of the basin. The deepest portion of the basin as determined from the seismic data coincides with


FIGURE 4
BOUGUER GRAVITY
SCALE IN MILES
0 1 2 3 4 5 6 7 8 9 10
CONTOUR INTERVAL : 10 MGAL
⑦ ..... : SEISMIC LINE
BOUGUER DENSITY=2.32/cc
— — — : INTERMEDIATE CONTOURS
PEARL ISLANDS
N
940,000
920,000
900,000
880,000
860,000
680,000
700,000
720,000
740,000
760,000
780,000

the area of lowest Bouguer gravity values: between lines 7 and 13 on the north and south and between lines 6 and 14 on the east and west. To the northwest of this gravity minimum, the Bouguer field increases in the direction of uplift toward the shore of western Panama. Northeast of the gravity minimum the Bouguer gravity values increase across a normal fault that is upthrown to the north. The fault is located near the intersection of lines 5 and 14. The northeast-southwest trending gravity low in this area corresponds to a shallow sedimentary trough. To the east, the Bouguer gravity increases in the direction of the uplift of the Pearl Islands. To the south, the Bouguer gravity increases toward the continental shelf where uplift of the basin occurred along the shelf edge.

East of line 16 and between lines 17 and 21 is a prominent east-west trending gravity high. This gravity high corresponds to the large uplifted block mapped on the Eocene horizon at this same location (Figure 3, Plate I).

A small localized gravity high exists at the intersection of lines 6 and 13 and is associated with an anticline. However, this anticline is displaced from the gravity high and no cause for the gravity maximum can be seen on either line 8 or line 13.

The sparse gravity data in the eastern part of the basin shows only that from the deepest part of the basin near the north end of line 26, the Bouguer gravity field increases to the south where the basin was uplifted at the

continental shelf edge.

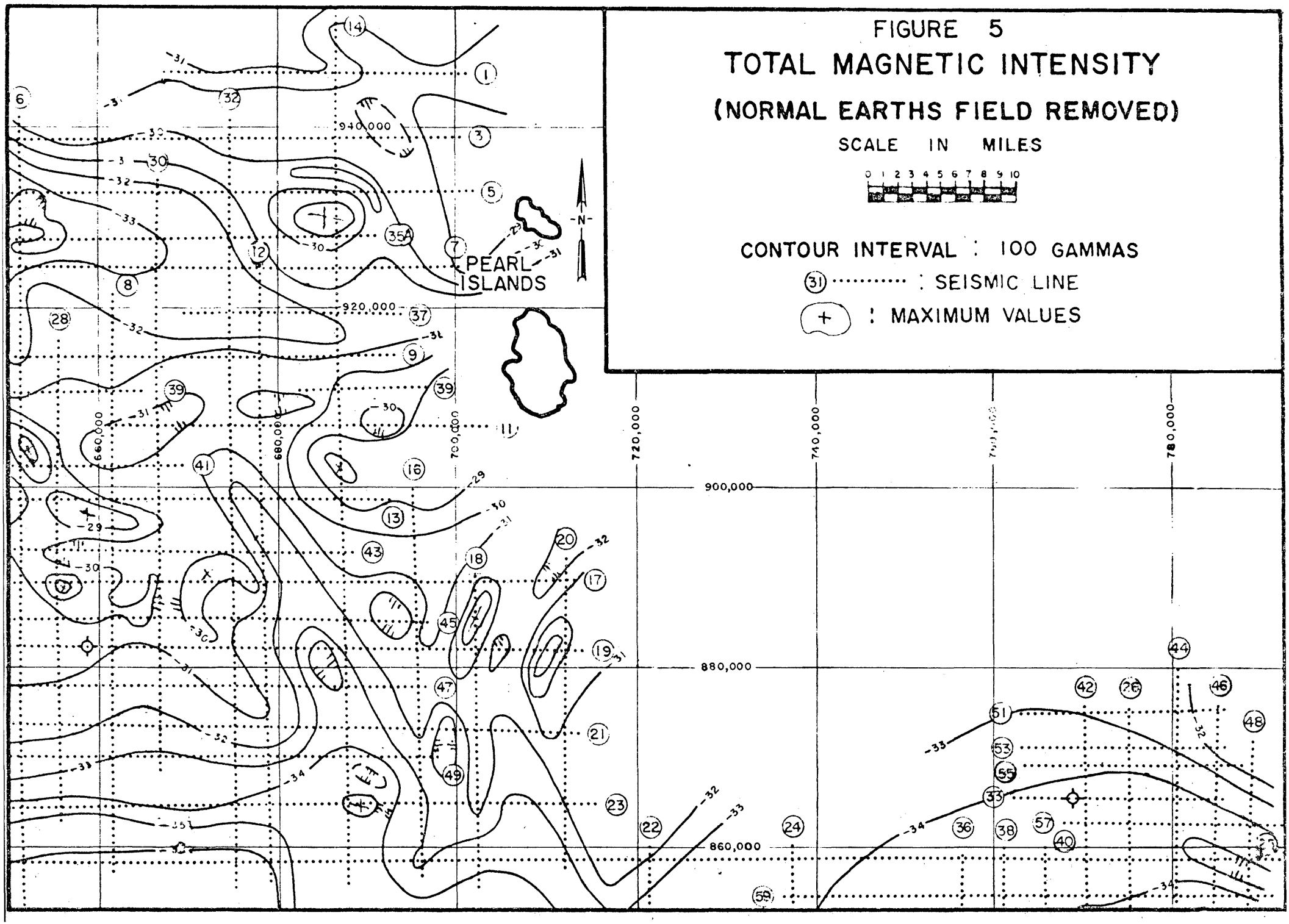
Between the eastern part and western part of the basin is a north-south trending gravity high. This gravity high corresponds to the uplifted ridge separating the eastern part of the basin from the western part.

Total Magnetic Intensity Data

The total intensity magnetic field map (Figure 5) was prepared by subtracting the earth's normal field from the total magnetic intensity recorded on the seismic ship. The data were contoured on a 100 gamma interval.

The difference between the sediments of the eastern part of the basin and the western part is clearly seen on the total magnetic intensity map. The eastern part lacks any local magnetic anomalies while the western part has many local anomalies. The relatively shallow Eocene sediments of the western part of the basin consist primarily of volcanic derived rocks. Therefore, the local magnetic anomalies could result from lateral variations in the magnetic susceptibility of the sediments. Some of the local anomalies appear to be caused by igneous intrusions. The magnetic anomalies at the intersection of lines 8 and 13 and at the intersection of lines 6 and 11 correspond to gravity maximums. The anomaly at the intersection of lines 6 and 11 also coincides with an anticline in the Eocene sediments. The anomaly at the intersection of lines 8 and 13 is associated with an anticline at the intersection of lines 6 and 13.

COLORADO SCHOOL OF MINES LIBRARY


FIGURE 5
TOTAL MAGNETIC INTENSITY
(NORMAL EARTHS FIELD REMOVED)
SCALE IN MILES
0 1 2 3 4 5 6 7 8 9 10
CONTOUR INTERVAL : 100 GAMMAS
(31) ..... : SEISMIC LINE
(+) : MAXIMUM VALUES
PEARL ISLANDS
N
940,000
920,000
900,000
880,000
860,000
660,000
680,000
700,000
720,000
740,000
760,000
780,000

At the intersection of lines 5 and 14 is a magnetic anomaly which coincides with an uplifted block. From this anomaly to the northwest is a region of high magnetic intensity which corresponds with the upfaulted block interpreted on the seismic data.

The magnetic anomaly on line 14 between lines 11 and 13 corresponds to a gravity maximum at the intersection of lines 14 and 11. An anticline exists in the Eocene sediments at this location.

In the vicinity of the intersection of lines 18 and 20 with lines 17 and 19 are several local anomalies. These anomalies are superimposed on an area of relatively high total magnetic intensity that corresponds to the large anticline that can be seen on the seismic data (Figure 3, Plate I). The anomaly at the intersection of lines 18 and 17 is coincident with a probable intrusive feature.

The magnetic and gravity features that have been described are summarized in Table 1 and are compared with corresponding features observed on the seismic data. A quantitative analysis of the gravity and magnetic data was not undertaken because of the limited scope of this investigation.

Seismic Velocities

The seismic velocity information provided by the geophone surveys from the Corvus #1 and Plaris #1 wells is summarized in Tables 2 and 3. A comparison of the interval

Table 1. Gravity and Magnetic Features

Location	Gravity Description	Magnetic Description	Seismic Description
Between lines 6 and 14 lines 7 and 13	Broad Gravity Minimum	Area of Low Magnetic Field Intensity	Deepest Part of Basin
North of line 7 west of line 14	Gravity Field Increases to Northwest	Magnetic Field Increases to North	Regional Uplift on Northeast Edge of Basin
Intersection of lines 3 and 14	Gravity Low		Shallow Sedimentary Trough
Between lines 17 and 21 east of line 16	East-West Trending Gravity High	Local Magnetic Anomaly	Large Anticlinal Uplift
Intersection of lines 8 and 13	Local Gravity Maximum	Local Magnetic Anomaly	No Expression

Table 2. Plaris #1 Velocity Summary

Depth K.B.	Depth S.L.	Delta D	Time S.L.	Delta T	Avg. Vel.	Int. Vel.
900	869		.1698		5118	
		700		.1075		6512
1600	1569		.2773		5658	
		300		.0483		6211
1900	1869		.3256		5740	
		600		.0914		6565
2500	2469		.4170		5921	
		550		.0858		6410
3050	3019		.5028		6004	
		100				
3150	3119					
		250				
3400	3369		.5551		6069	
		100				
3500	3469					
		800				
4300	4269		.6809		6270	
		600		.0807		7435
4900	4869		.7616		6393	
		1500		.1956		7669
6400	6369		.9572		6654	
		600		.0605		9917
7000	6969		1.0177		6848	
		500		.045		11111
7500	7469		1.0627		7028	
		1300		.1037		12536
8800	8769		1.1664		7518	
		600		.0426		14085
9400	9369		1.2090		7749	

K.B. = Kelly Bushing

S.L. = Sea Level

D = Depth

T = Time

Avg. Vel. = Average Velocity

Int. Vel. = Internal Velocity

Table 3. Corvus #1 Velocity Summary

Depth K.B.	Depth S.L.	Delta D	Time S.L.	Delta T	Avg. Vel.	Int. Vel.
355	324		.0648		5000	
		345		.0671		5142
700	669		.1319		5072	
		800		.137		5839
1500	1469		.2689		5463	
		500		.0817		6120
2000	1969		.3506		5616	
		550		.0861		6388
2550	2519		.4367		5768	
		650		.0561		11586
3200	3169		.4928		6431	
		300		.021		14286
3500	3469		.5138		6752	
		150		.0138		10870
3650	3619		.5276		6859	
		950		.0661		14372
4600	4569		.5937		7969	
		1000		.070		14286
5600	5569		.6637		8391	
		400		.0255		15686
6000	5969		.6892		8661	
		1600		.1115		14350
7600	7569		.8007		9453	
		980		.0552		17754
8580	8549		.8559		9988	

K.B. = Kelly Bushing

S.L. = Sea Level

D = Depth

T = Time

Avg. Vel. = Average Velocity

Int. Vel. = Internal Velocity

velocities from the wells with the lithologies shows that the seismic velocity in the high volcanic Eocene sediments ranges from 11,000 to 15,000 feet per second while the velocity of the Miocene and Pliocene sediments ranges from 6000 to 10,000 feet per second. This contrast in velocity provides a clear method for using the seismic data to distinguish between Miocene and Pliocene sediments and older sediments.

Seismic velocities have been determined from the velocity versus reflection time displays that are produced during the procedure of obtaining stacking velocities for CDP families. This method of velocity determination produces a stacking velocity that is not the true average velocity. The velocities determined from the geophone well survey are the average velocities. For practical application the ratio of average velocity to stacking velocity will be assumed constant. Table 4 shows the determination of the ratio of average to stacking velocity at the Plaris well location. All references to velocity in this discussion is to the average velocity using the ratio of average to stacking of .98.

The velocity contrast between Eocene and younger sediments may explain why deep reflections are not observed over most of the area of the western part of the basin (Figure 6). In the Corvus #1 well, the reflection coefficient at the unconformity between Pliocene and Eocene sediments is .41. This large reflection coefficient means that the amount of energy that is transmitted to the older section

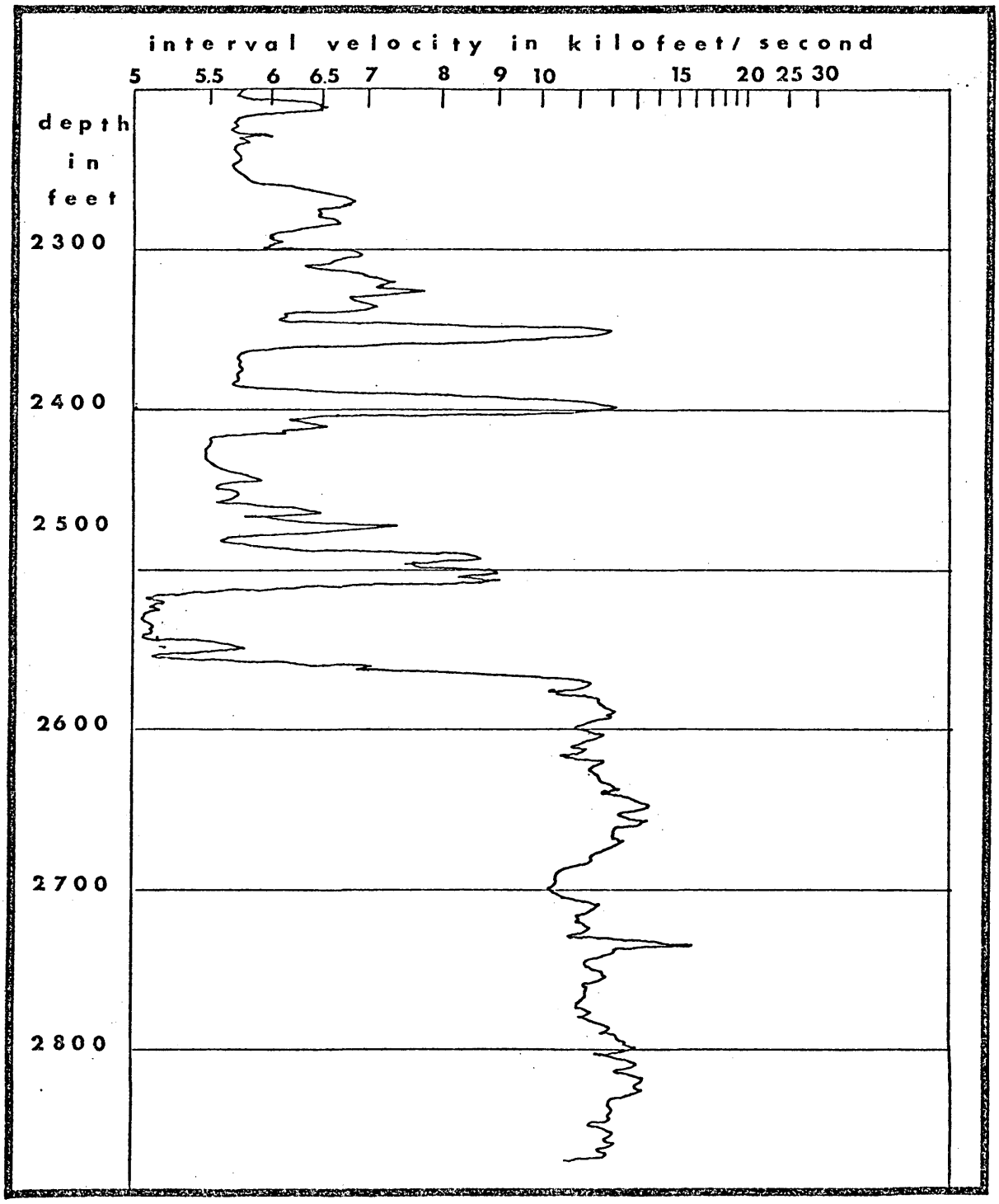


FIGURE 6: CALIBRATED VELOCITY LOG CORVUS WELL

Table 4. Velocity Analysis Calibration

Reflection Time	Airgun Velocity	Velan Velocity	Airgun/Velan
		Plaris #1	
.65	5740	5625	1.000
1.05	6004	6025	.996
1.41	6270	6500	.960
		Corvus #1	
.992	5768	5900	.978
1.42	8661	8850	.979
1.81	9988	9350	1.000

and transmitted back through the unconformity is not sufficient to produce reflections on the seismic record that are distinguishable from inherent noise.

The seismic velocities below the unconformity in the western part of the basin are in the range of velocities of the Eocene sediments encountered in the Corvus #1 well. No coherent reflections are observed below 2.0 seconds anywhere in the western part of the basin and in many places only very weak reflections are observed immediately below the unconformity. These two factors indicate that only highly volcanic Eocene sediments are preserved below the unconformity in the western part of the basin.

Interpretational Limitations

The lithology and age of the sediments of the Gulf of Panama basin are known at only the locations of the Corvus and Plaris wells. Conclusions that are made concerning the age and lithology of sediments elsewhere in the basin and conclusions concerning the age and mechanism of development of structures are therefore dependent upon the interpretation of seismic, gravity, and magnetic data. All conclusions must be considered in view of the limitations that the data impose on the interpretation.

The limitations which are most directly related to the conclusions of this study stem from the interpretation of the seismic data. In the western part of the basin, the age of sediments below the unconformity is interpreted to

be Eocene since the velocity of these sediments is within the range of velocities for the Eocene sediments encountered in the Corvus #1 well. However, the lack of reflector continuity which precludes the accurate mapping of any one horizon also decreases the validity of the velocity analyses and limits the area over which the velocity analyses can be used. Despite the limitations of the velocity data, they provide the most reliable method of determining the age of sediments below the unconformity.

In the eastern part of the basin, the age of the unconformity is interpreted to be the end of Middle Miocene because of the thinning of Middle Miocene sediments across the top of the structure on which the Plaris well was drilled and because of the apparent angularity of Middle Miocene sediments below the Late Miocene sediments. However, no break in deposition can be determined from the paleontological data.

ARTHUR LAKES LIBRARY
COLORADO SCHOOL of MINES
GOLDEN, COLORADO 80401

PLATE TECTONICS

The structural development in the Gulf of Panama basin occurred in two episodes. The first episode is represented by the horst and graben system that created the Tuira-Chucunague Basin, the Bayano Basin, the Sambu Basin, the offshore basin in which the Plaris well was drilled and possibly other basins in the Gulf of Panama (Figure 1). The second episode is represented by the local folds and faults in the basins, which resulted from widespread uplift, deformation, and erosion, interpreted as occurring during Middle Miocene. The first episode is reminiscent of large scale rifting that is observed in the Red Sea (Lowell, et al., 1975). This indicates that at least during Oligocene through Early Miocene, the Nasca and Caribbean plates were diverging (Figure 7). Evidence for the present relative motions of the Nasca and Caribbean plates is inconclusive (Molnar, et al., 1969, and Case, et al., 1971). However, the absence of an oceanic trench bordering the continental shelf of the Gulf of Panama is consistent with divergence of the two plates.

The Middle Miocene episode of deformation cannot be conclusively interpreted as resulting from uplift and rifting attendant with divergence of the Nasca and Caribbean plates. The predominance, perhaps exclusivity, of normal faulting and the basement fault-block origin of most structures formed during this period, is indicative of divergent

plate motions according to proposed models of continental rifting and incipient ocean-floor spreading (Kinsman, 1975).

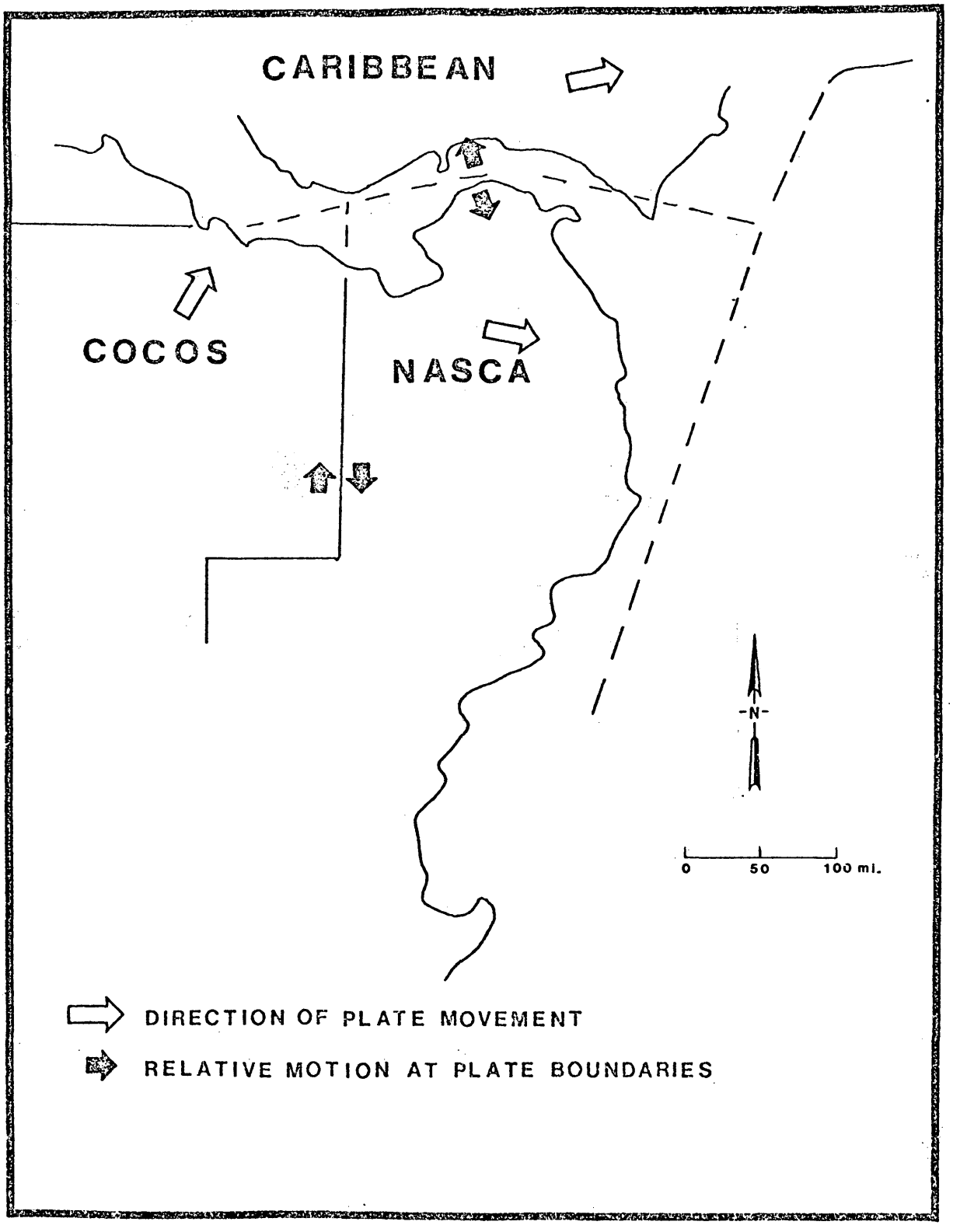


FIGURE 7: PLATE MOTION

CONCLUSIONS

Structure within the Tertiary sediments of the Gulf of Panama basin developed in the following sequence:

I. Sediments with a high percentage of volcanic clastic constituents were deposited in the basin in Eocene and part of Early Miocene time.

II. Horst blocks which localized sediment deposition began forming during Eocene time and the Gulf of Panama basin became a system of horst-bounded sedimentary basins.

III. Marine sediments free of volcanic constituents were deposited throughout late Early Miocene and Middle Miocene time. The limit of deposition of these sediments extended farther south and west than the present limit of their occurrence and the area of deposition may have occupied the entire Gulf of Panama.

IV. At approximately the end of Middle Miocene time, the entire basin of the Gulf of Panama was uplifted. In the western part of the basin, all Miocene and Late Eocene sediments were removed by erosion.

V. In the eastern part of the basin, Middle and Early Miocene sediments were preserved.

VI. Prior to deposition of Late Miocene and younger sediments, most of the structures in the basin were formed. The structures can be genetically divided into two types:

1. Basement fault blocks.
2. Igneous intrusions.

VII. Deposition of Late Miocene sediments was restricted to the eastern part of the basin. The anticline on which the Plaris #1 well was drilled, continued developing during Late Miocene.

VIII. During Pliocene time the entire basin began to subside and no further structural development occurred except for minor faulting.

The history of structural development in the Gulf of Panama is consistent with the history of the onshore structure in eastern Panama. Structure development in the Gulf occurred during Middle Miocene time coinciding with the time of structural development in the basins of eastern Panama. The Gulf of Panama basin can therefore be grouped with the eastern Panama basins as part of the Bolivar Geosyncline of northern South America.

The eastern part of the basin is of the same type as the eastern Panama basins. The western part of the basin appears to contain two individual basins, also similar to the basins of eastern Panama, but altered in appearance by the Middle Miocene uplift.

The horst and graben origin of the basins of Panama, both on and off shore, are the result of divergence of the Nasca and Caribbean lithospheric plates during Oligocene to Early Miocene time. The Middle Miocene deformation may have resulted from rifting and taphrogenesis during divergence of the Nasca and Caribbean plates. Some of the structure has been formed by igneous intrusions and one anticline is either a slump feature or a diapiric feature.

Table 5. Sedimentary and Tectonic Events

Geologic Age	Western Part of Basin	Eastern Part of Basin	Onshore Basins
Middle Eocene	Formation of horst and graben basins deposition of volcanic sediments	Formation of horst and graben basins deposition of volcanic sediments	Formation of Bolivar Geosyncline
Late Eocene	?	?	
Oligocene	?	?	End of volcanism, start of marine transgression
Early Miocene	?	End of volcanic sedimentation	
Middle Miocene	Uplift and erosion	Uplift and erosion	
Late Miocene		Subsidence	Uplift and erosion
Pliocene	Subsidence		

BIBLIOGRAPHY

Case, J. E., Duran, L. G., Lopez, Alfonso, and Moore, W. R., 1971, Tectonic investigations in Western Colombia and Eastern Panama: Geol. Soc. America Bull., v. 82, p. 2685.

Dix, C. Hewitt, 1955, Seismic Velocities from Surface Measurements: Geophysics, v. 20, no. 1, p. 68.

Dobrin, Milton B., 1960, Geophysical Prospecting: McGraw-Hill Book Company Inc., New York.

Fisher, R. L., 1974, Pacific-Type Continental Margins: p. 25 in The Geology of Continental Margins, Edit. Burke, C. A., and Drake, C. L., Springer-Verlag.

Johnson, M. S., and Headington, Edward, 1971, Panama: Exploration History and Petroleum Potential: Oil and Gas Jour., v. 51, p. 96.

Kinsman, D. J. J., 1975, Rift Valley Basins and Sedimentary History of Trailing Continental Margins: p. 83-126, in Petroleum and Global Tectonics, Edit. Fischer, A. G. and Judson, S., Princeton Univ. Press.

Lowell, J. D., Genik, G. J., Nelson, T. H., and Tucker, P. M., 1975, Petroleum and Plate Tectonics of the Southern Red Sea, p. 129-153 in Petroleum and Global Tectonics, Edit. Fischer, A. G. and Judson, S., Princeton Univ. Press.

Molnar, Peter, and Sykes, Lynn R., 1969, Tectonics of the Caribbean and Middle America Regions from Focal Mechanisms and Seismicity: Geol. Soc. America Bull., v. 80, p. 1639-1684.

Nygren, W. E., 1950, Bolivar Geosyncline of Northwestern South America: Am. Assoc. Petroleum Geologists Bull., v. 34, no. 10, p. 1998.

Sheriff, R. E., ed., 1974, Encyclopedic Dictionary of Exploration Geophysics: Soc. Explor. Geophysicists, Tulsa, Oklahoma.

Shor, G. G., Jr., 1974, Continental Margin of Middle America: p. 599, in The Geology of Continental Margins, Edit. Burke, C. A. and Drake, C. L., Springer-Verlag.

Terry, R. A., 1956, A Geological Reconnaissance of Panama: California Acad. Sci., no. 23.

Van Andel, T. J., Heath, G. R., Malfait, B. T., Heinrichs, D. F., and Ewing, J. I., 1971, Tectonics of the Panama Basin, Eastern Equatorial Pacific: Geol. Soc. America Bull., v. 82, p. 1489.